Journal of Solar Energy Research (JSER)

Journal homepage: jser.ut.ac.ir

Frequency Control and Power Balancing in a Hybrid Renewable Energy System (HRES): Effective Tuning of PI Controllers in the Secondary Control Level

Mohsen Aryan Nezhad [a, *]

[a]*Department of Electrical Engineering, Faculty of Electrical and Computer Engineering, Technical and Vocational University (TVU), Tehran, Iran.*

Received: 2021-09-06
Accepted: 2022-01-02

Abstract

With advent of the modern Hybrid Renewable Energy System (HRES), the application of different energy storage systems has increasingly expanded. When the solar radiation or wind speed has low values, the energy storage system (ESS) injects the required energy to supply the load demand, continuously. Due to large numbers of equipment and different control loops in the HRES, effective contribution of ESS needs an efficient control approach to coordinate the ESS with other equipment within HRES. To fulfil this gap, a Proportional Integral (PI)-based control synthesis approach is presented for the tuning of the PI controllers. In the proposed method, all PI controllers for different types of ESS are designed based on root-locus trajectory, damping coefficient of dominant poles, and coordination among different equipment. Finally, comparison among different types of ESS based on presented control approach is performed. Results show that the presented control technique has adequate capability to damp the frequency deviations against multiple disturbances and parameter variations.

Keywords: Damping Coefficient of Dominant Poles, Energy Storage System (ESS), Hybrid Renewable Energy System (HRES), Wind Turbine (WT).

1. Introduction

With a reduction in the wind speed or solar radiation, power production of PV and WT seriously reduces [1]. Therefore, the MG power balancing between production and consumption is disrupted and the MG frequency can change out of its nominal range [2]. To improve the MG stability, an ac MG consists of different levels of control loops such as local, secondary, and global controls [3]. The local control manages primary control such as current and voltage control loops in the MS [4]. The secondary control ensures that the frequency and voltage deviations of the MG are in the permitted range after every change in load or supply [5]. The global control, beside economic power management, can perform technical roles like; connect/disconnect of the MG, load-shedding in emergency mode, optimal power flow between different MGs and grid, monitoring and providing of the voltage and frequency setpoints for the MGs to synchronize with the main grid [5].

Renewable resources are irregular energy providers that their power generation cannot be exactly predicted [6]. Therefore, for covering uncertainties of renewable resources, such resources can be integrated with conventional power providers like the DG and this combination create the HRES [7]. So, the HRES is one type of the MG that

* m-aryannezhad@tvu.ac.ir

renewable resources, and conventional power providers are used together [8].

To keep power balancing between production and consumption immediately, participation of ESS beside the DG is essential to control the frequency of the HRES under severe disturbances [9]. A method for energy storage is passing a direct current through the SC and storing it permanently in a magnetic field [10]. A cost-effective and economical model of the SC is the HTS that is usually cooled by liquid nitrogen or liquid helium and due to advanced manufacturing technology; the SMES can quickly empty its total energy. Also, its lifetime is not affected by the number of charges, discharges, and duration of the energy storage. Moreover, due to the absence of moving parts, the SMES is extremely high reliable [11].

The FESS is a rotating mechanical device that is used for storing of rotational energy for a long time [12]. Due to the simple structure of the FESS which is based on high speed rotating mass, the FESS has many benefits such as safety, not being constrained by fixed temperature limit, no lifetime degradation of performance, environmental compatibility; low maintenance costs and has a high predictable lifetime than other energy storage devices [12].

To keep fast power balancing against load variations, the contribution of fast energy storage systems like UC is crucial [13]. The UC supplies a huge amount of energy in a short time and controls the frequency of the islanded system under severe disturbances [8].

Recently, many investigations have been performed to improve the MG frequency stability. In [14], to enhance the stability and improve the flexibility of the MG frequency in islanded mode, a PSO-based fuzzy method is presented for the tuning of the PI controller and the results are compared with a conventional PI controller tuned by Ziegler-Nichols method. In [15], a new fuzzy logic pitch controller is designed to reduce power fluctuations of the WT during the MG islanded mode, and results are compared with a PI controller. In [16], for extracting maximum power under unbalanced weather conditions a new method is presented for the design of Takagi–Sugeno fuzzy-based controller. In [17], different types of the ESS in the MG are examined considering arrangement, topology, power electronic interfaces, control schemes, control strategy, potential trends, and challenges of the ESS. In [18], the hierarchical control and islanded operating of the MG are investigated and a summary of the control strategy is discussed considering reserve conditions of the DGs, loads, and ESS. In [19], the fuzzy control and PSO algorithm are used to reach the charge/discharge mode and the amount of energy in the ESS in each hour of a day.

Although the use of complex methods for the load frequency control of the HRES is developed and such methods usually evaluate their results with the conventional PI controllers, but such conventional PI controllers normally are not efficiently tuned. Because the use of complex controllers often cannot be implemented due to heavy performance costs and design complexity, this paper addresses the tuning of the secondary controllers of the HRES considering root-locus trajectory and coordination among local and secondary controllers. For this purpose, different scenarios for an isolated ac HRES are considered. For enhancing the frequency stability, a PI controller in the secondary control level provides a control signal for the ESS considering coordination among different equipment to cover lack of the energy in a short time. Then, the HRES frequency deviations are simulated considering multiple random disturbances and parameter variations. According to the obtained results, the design of the local and secondary controllers based on the presented method has sufficient potential to overcome the HRES control challenges like; load fluctuations, and parameter variations.

This paper is organized as follows: Section 2 illustrates a mathematical method for providing of proper damping coefficient based on the root locus approach. In Section 3, dynamic models of the WT, DG, and ESS are presented. The proposed control strategy and obtained results are discussed in Section 4. Finally, the conclusions are presented in Section 5.

2. Root locus-based control synthesis

Using the root locus method, it could be possible to obtain the trajectory of the closed-loop system roots as a function of the feedback gain. This method is used to investigate the gain changes on the location of the closed-loop poles [20]. To design a controller based on the root locus method, it is necessary to obtain transfer functions between considered input and output, and feedback of the system [21].

The root locus of the closed-loop characteristic can be obtained for changes of the feedback gain $0 \le k \le +\infty$. So, the closed-loop transfer function is:

$$\frac{y(s)}{u(s)} = \frac{G(s)}{1 + kG(s)F(s)} \quad (1)$$

where, G(s) is the transfer function between desired input and output, F(s) is the feedback transfer function and *k* is the controller gain. Therefore, the closed-loop poles for given *k* is determined by:

$$1 + kG(s)F(s) = 1 + k\frac{s^n + a_{n-1}s^{n-1} + ... + a_0}{s^m + b_{m-1}s^{m-1} + ... + b_0} = 0 \quad (2)$$

Or

$$G(s)F(s) = \frac{-1}{k} \quad (3)$$

According to (3), the root locus trajectory of each case study presents all real values of the feedback gain [21]. With obtaining the G(s) and F(s) in a practical model, one can select the feedback gain, *k*, so that dominant poles of the closed-loop system lie in the proper region.

According to Fig. 1, if the dominant poles of the closed-loop system lie in the region of $0.4 \le \xi \le 0.8$ and $t_s \le \frac{4}{\xi\omega_n}$ of the complex plane, the designed controller quarantines a good performance for the closed-loop system. To have low frequency deviations with fast response, the PI parameters like K_P and K_I are obtained based on the damping coefficient of dominant poles, ξ, and system natural frequency, ω_n.

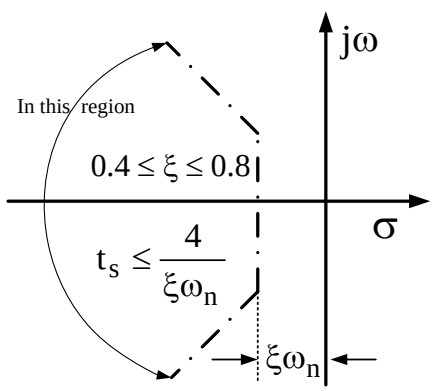

Figure 1. Proposed control strategy for tuning of secondary controllers

In this case, the control target is to choose the controller parameters so that the HMG has the desired damping coefficient. This method is used to place the closed-loop dominant poles on a suitable location, and improve the damping of the system, efficiently. Interested readers can find more details about root-locus details in [21].

3. HRES dynamic modelling

The HRES usually consists of the WT, and DG. The DG works as the main part of the HRES for frequency control. The input of the DG is the load variations and the output is the load frequency changes [22]. As shown in Fig.2. A, the valve actuator and diesel engine are modelled with the first-order transfer functions and time constants T_{sm} and T_d. Inertia is shown by H_d and the governor includes droop constant (R), and integral controller [22]. For a suitable response, the droop value of DG is selected between 3% to 7% to avoid undesirable frequency error in steady-state conditions [22]. The integral controller eliminates this steady-state error. But, this issue reduces the stability margin and makes more oscillations in the load frequency [22].

The power production of WT depends on wind speed V (m/s), and it changes as a cubic function. The mechanical power of the WT can be obtained by:

$$P_{WT} = \frac{1}{2}\rho A_r C_p V^3 \quad (4)$$

where, ρ is the air density (kg/m3), A_r is the swept area of blade (m^2), C_p is a coefficient that changes as a function of tip speed ratio (λ) and blade pitch angle (β). The WT dynamic model includes the low-speed shaft, high-speed shaft, hydraulic pitch control, and fluid coupling transfer functions as shown in Fig. 2. B [23, 24]. The WT kinetic energy can be used for the HRES frequency control. For this purpose, the load frequency deviations are directly applied to the DG control loop and WT pitch loop [25].

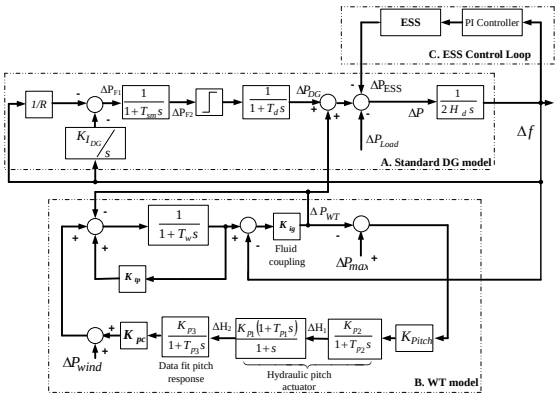

Figure 2. The HRES dynamic model

In case of any change in the load demand or weather condition, the power balancing can be simply disrupted. In this case, the DG unit uses the valve actuator and diesel engine for injection of energy and damping of the frequency deviations [22]. For severe disturbances occurred in a short time, the DG cannot inject a lot of energy because of the mechanical process and heat rate of the diesel engine. Because the HRES components like DG, and WT have a slow nature, it is interesting to use high-speed ESS like UC, SMES, and FESS in the hybrid system as shown in Fig. 2. C. To efficiently track the frequency deviations occurred in the HRES, contribution of the ESS for the load frequency control is essential. Because of the quick injection of internal energy, the ESS like the SMES, UC, and FESS are modelled with the first-order transfer functions with the time constant $T_{smes}, T_{UC}, \text{and } T_{FESS}$ respectively [14, 26]. In this case, the SMES, UC, and FESS transfer functions are formulated in (5, 6, and 7). The HRES and ESS parameter values are given in the appendix [14, 22-26].

$$ESS = \begin{cases} \dfrac{1}{1+T_{SMES}s} & (5) \\ \dfrac{1}{1+T_{UC}s} & (6) \\ \dfrac{1}{(1+T_{FESS}s)} & (7) \end{cases}$$

4. Results & Discussion

Low power generation of the renewable resources or load demand rising can easily disrupt the power balancing of the HRES [27]. Therefore, to support the load demand and make power balancing in a short time, real-time frequency control of the HRES equipped by the ESS is necessary. For this purpose, as shown in Fig.2.C, the PI controller, and the ESS cover the lack of energy, immediately. In this case, for obtaining the locus of the HRES poles calculation of the G(s) and F(s) is necessary. To make the typical type of the closed-loop system shown in Fig. 2, it is necessary to find the feedforward and feedback transfer functions of the HMG. The feedback transfer function of HMG is the ESS control loop, and the remaining of HMG model is a feedforward transfer function. According to Fig. 2. A, and B, the G(s) is the transfer function between ΔP_{load} and Δf can be obtained as:

$$G(s) = \frac{-0.3333s^7 - 20.67s^6 - 453.6s^5 - 4325s^4 - 18610s^3 - 30600s^2 - 14750s}{s^8 + 62.51s^7 + 1391s^6 + 13980s^5 + 75710s^4 + 270000s^3 + 702400s^2 + 586000s + 132700}$$

Transfer function of the feedback loop, F(s), is the ESS transfer function which is given in (5, 6, and 7). Considering obtained G(s) and F(s), the root locus of the HRES equipped by SMES, UC, and FESS are shown in Figs. 3, 4, and 5.

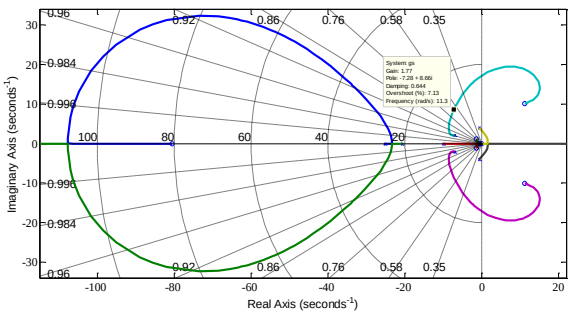

Fig. 3 Root-locus trajectory of the HRES equipped by FESS

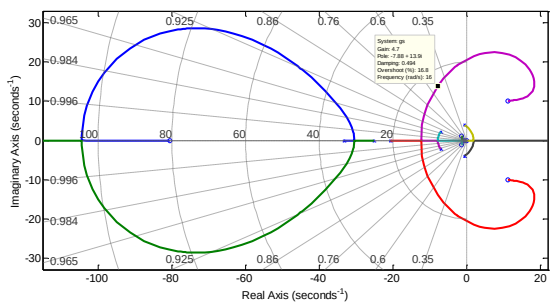

Fig. 4 Root-locus trajectory of the HRES equipped by SMES

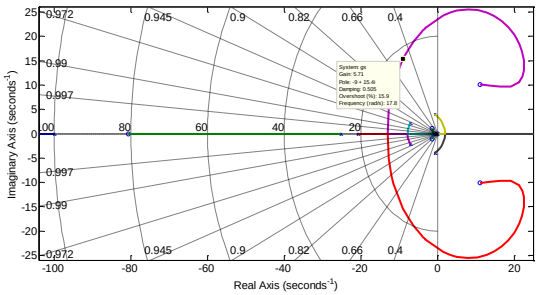

Fig. 5 Root-locus trajectory of the HRES equipped by UC

In this case, the selection of the gain value for the proportional controller is based on proper control condition as shown in Fig. 1. For FESS, the gain value is equal to 1.77. So, the settling-time of the HRES dominant poles is $t_s \le \frac{4}{\zeta\omega_n} = \frac{4}{0.644\times 11.3} = 0.55$ (s). For SMES, the gain value and settling-time are equal to 4.7 and 0.48 (s). For UC, the gain value and settling-time are equal to 5.71 and 0.445 (s). To enhance the system response and remove the steady error, the integral controller coefficients for FESS, SMES, and UC are selected 8, 9, and 11, respectively. Although bigger or lower values can be selected for proportional gains, but lower value results a slower response and a bigger value gives a faster response with higher oscillations. So, these selected values for proportional gains are trade-off between fast responses and output oscillations. As well, the integral coefficients are selected via try and error. Any change in load demand can easily disrupt the power balancing of the HRES. Therefore, according to the obtained values, the step response of the HRES for 0.1 (p.u) load increase is as shown in Fig 6. To show the effectiveness of the proposed approach, the step response of the system against 0.1 (p.u) load increase for ±50% parameter changes in all parameters, given in Appendix, is also shown in Figs. 7 and 8.

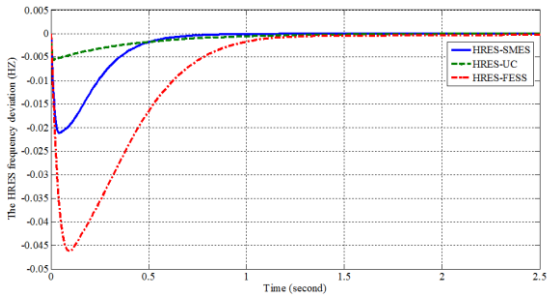

Fig.6 Step response of the HRES for 0.1 load increase under nominal parameters

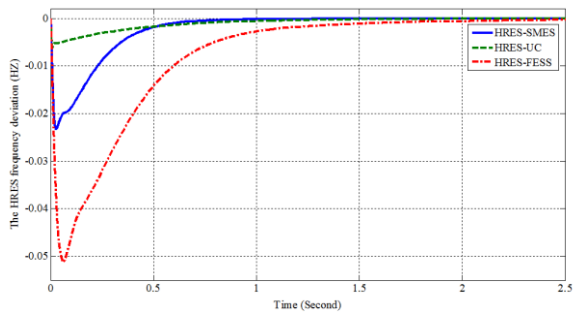

Fig.7 Step response of the HRES for 0.1 load increase for +50% changes in all HRES parameters

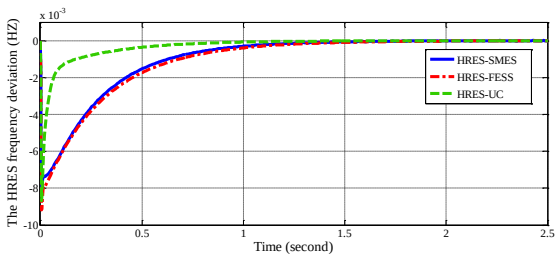

Fig.8 Step response of the HRES for 0.1 load increase for -50% changes in all HRES parameters

As shown in Figs. 6, 7, and 8, the HRE equipped by fast ESS can create load balancing in a short time and damp frequency oscillations in nominal and changed parameters, effectively. To show the effectiveness of the secondary control loop performance in frequency stability, the step responses of the HRES without ESS control loop are obtained as shown in Fig 9, and 10.

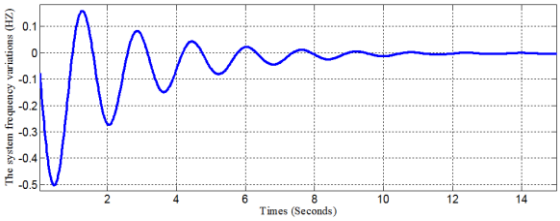

Fig.9 Step response of the HRES for 0.1 load increase under nominal parameters without ESS control loop

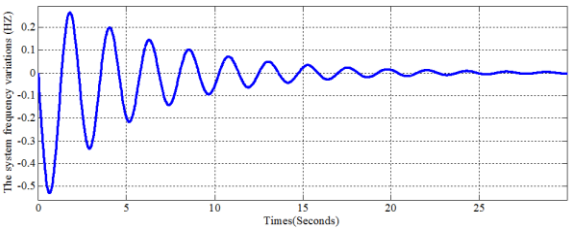

Fig.10 Step response of the HRES for 0.1 load increase for +50% parameter changes in all HRES parameters without ESS control loop

As shown in Figs. 9, and 10, the islanded system has high frequency oscillations and DG/WT system cannot effectively provide the power balancing. Since the system components like DG, and WT have a slow nature, the islanded system cannot damp the frequency oscillations, effectively.

The load demand has an irregular behaviour and can change randomly. In this case, under random load variations shown in Fig. 11, the load frequency variations are obtained as presented in Figs. 12 and 13.

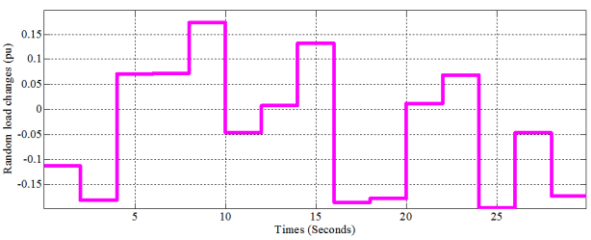

Fig. 11 Random load variations

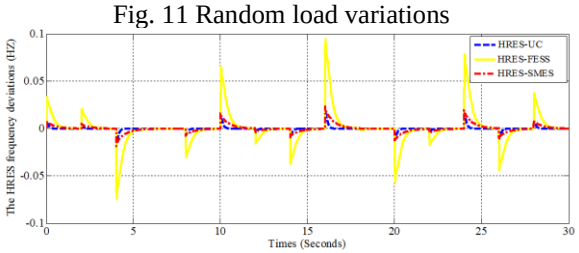

Fig.12 Frequency variations of the HRES under random load changes for nominal parameters

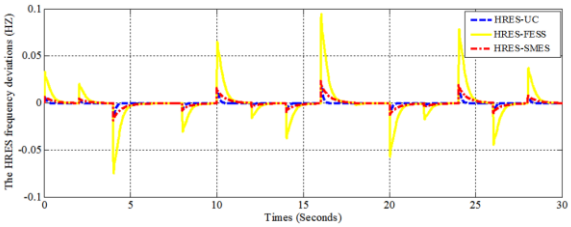

Fig.13 Frequency variations of the HRES with random load changes for +50% parameter changes in all HRES parameters

According to Figs. 12 and 13, presented control strategy with the participation of the UC, SMES, and FESS in the secondary loop considerably improves the frequency stability of the HRES against random load disturbances and parameter variations.

5. Conclusions

The PI parameters can be achieved based on the appropriate value of the damping coefficient of the HRES dominant poles. It can be used as a suitable technique for coordination of the HRES components and tuning of the controllers. This control strategy has sufficient potential to efficiently damp the HRES frequency oscillations. According to the obtained results, presented control method with contribution of rapid ESS in the secondary control level can considerably improve frequency stability; provide coordination among the HRES components and robustness of the HRES against parameter variations.

Nomenclature

DG	Diesel Generator
DGs	position of
ESS	Energy Storage Systems
FESS	Flywheel Energy Storage Systems
HRES	Hybrid Renewable Energy Systems
HTS	High-Temperature Superconductor
IC	Interconnection Device
Ki	Integral Coefficient
MGs	Microgrids
MS	Microsources
PV	Photovoltaic Panels
PI	Proportional – Integral
PSO	Particle Swarm Optimization
SMES	Superconducting Magnetic Energy Storage
SC	Superconducting Coil
UC	Ultracapacitor
WT	Wind Turbine

APPENDIX

All parameter values are expressed in p.u on a base power of 500 (kW).

DG:

Rated power= 500 (kW),

$H_d = 1.5,\ T_d = 0.5\,(\text{Sec}),\ T_{sm} = 0.05\,(\text{Sec}),\ f = 60\,(\text{HZ})$

WT:

Rated power= 500 (kW-AC),

$T_w = 4(\text{Sec}),\ K_{pc} = 0.08,\ K_{p1} = 1.25,\ K_{p2} = 1,$

$K_{p3} = 1.4,\quad K_{ig} = 1.494,\ T_{p1} = 0.6(\text{sec}),\ T_{p2} = 0.041(\text{sec}),$

$T_{p3} = 1(\text{sec}),\ K_{tp} = 0.004,$

SMES, UC, and FESS:

$T_{SMES} = 0.03(\text{sec}),\ T_{UC} = 0.01(\text{sec}),\ T_{FESS} = 0.1(\text{sec}),$

References

1. AbubakarShaabana;, H.R.E.-H.M.S.Y., *Decomposition based multiobjective evolutionary algorithm for PV/Wind/Diesel Hybrid Microgrid System design considering load uncertainty.* Energy Reports, 2021. **7**: p. 52-69.
2. Lasseter, R., et al., *The CERTS microgrid concept [J]. White paper for Transmission Reliability Program, Office of Power Technologies, US Department of Energy, 2002, 2 (3): 30.* Google Scholar.
3. Bevrani, H., M.R. Feizi, and S. Ataee, *Robust Frequency Control in an Islanded Microgrid: ${H} _ {\infty} $ and $\mu $-Synthesis Approaches.* IEEE transactions on smart grid, 2016. **7**(2): p. 706-717.
4. Ali Rafinia, J.M., Navid Rezaei,, *Towards an enhanced power system sustainability: An MILP under-frequency load shedding scheme considering demand response resources,*
. Sustainable Cities and Society, 2020. **59**.
5. Bevrani, H., B. François, and T. Ise, *Microgrid dynamics and control*. 2017: John Wiley & Sons.
6. Mohammad Fathi, a.H.B., *Adaptive Energy Consumption Scheduling for Connected Microgrids Under Demand Uncertainty.* IEEE Transaction on Power Delivery, 2013. **28**.
7. Nezhad, M.A. and H. Bevrani, *Frequency control in an islanded hybrid microgrid using frequency response analysis tools.* IET Renewable Power Generation. **12**(2): p. 227-243.
8. Nezhad, M.A. and H. Bevrani, *Real-time AC voltage control and power-following of a combined proton exchange membrane fuel cell, and ultracapacitor bank with nonlinear loads.* International Journal of Hydrogen Energy, 2017. **42**(33): p. 21279-21293.
9. Vallem V. V. S. N. Murty, A.K., *Optimal Energy Management and Techno-economicAnalysis in Microgrid with Hybrid RenewableEnergy Sources.* Journal of modern power systems and clean energy, , 2020. **8**.
10. Kim, A.-R., et al., *SMES application for frequency control during islanded microgrid operation.* Physica C: Superconductivity, 2013. **484**: p. 282-286.
11. Kim, A., et al., *A feasibility study on HTS SMES applications for power quality enhancement through both software*

simulations and hardware-based experiments. Physica C: Superconductivity, 2011. **471**(21): p. 1404-1408.
12. Francisco Díaz-González, A.S., OriolGomis-Bellmunt, Fernando D.Bianchi, *Energy management of flywheel-based energy storage device for wind power smoothing*. Applied Energy, 2013. **110**: p. 207-219.
13. Nayeripour, M., M. Hoseintabar, and T. Niknam, *Frequency deviation control by coordination control of FC and double-layer capacitor in an autonomous hybrid renewable energy power generation system.* Renewable Energy, 2011. **36**(6): p. 1741-1746.
14. Bevrani, H., et al., *Intelligent frequency control in an AC microgrid: Online PSO-based fuzzy tuning approach.* IEEE transactions on smart grid, 2012. **3**(4): p. 1935-1944.
15. Rashad M.K, C.A., Nagasaka K, *Enhancement of micro-grid performance during islanding mode using storage batteries and new fuzzy logic pitch angle controller*. Energy Conversion and Management 2011: p. 2204-2216.
16. Malla S.G, B.C.N., *Enhanced operation of stand-alone "Photovoltaic-Diesel Generator-Battery" system.* Electric Power Systems Research 2014: p. 250-257.
17. Xingguo T, Q.L., Hui W, *Advances and trends of energy storage technology in Microgrid.* Electrical Power and Energy Systems 2013: p. 179–191.
18. Lin Y, H.B.S., Xu R.S, Li C.L, *Dynamic modeling of a hybrid wind/solar/hydro microgrid in EMTP/ATP Original Research Article.* Renewable Energy 2012: p. 96-106.
19. Darvishi A, A.A., Abdi B, *Optimized Fuzzy Control Algorithm in Integration of Energy Storage in Distribution Grids.* Energy Procedia, 2011: p. 951- 957.
20. JE, V.N., *Root loci of load frequency control systems.* Appl Syst 1963. **82**: p. 82:712–726.
21. K, S., *An alytical approach to root loci.* IRE Transaction on Automatic Control, 1961.
22. Papathanassiou, S.A. and M.P. Papadopoulos, *Dynamic characteristics of autonomous wind–diesel systems.* Renewable Energy, 2001. **23**(2): p. 293-311.
23. Tripathy S.C, K.M., Balasubramanian R. , *Stability Simulation and Parameter Optimization of a Hybrid Wind-Diesel Power Generation System.* International Journal of Energy Research, 1992. **16**: p. 31-42.
24. Tan, W. and J. Zhang. *Load frequency control for wind-diesel hybrid systems*. in *Control Conference (CCC), 2011 30th Chinese*. 2011. IEEE.
25. Agbossou, K., et al., *Performance of a stand-alone renewable energy system based on energy storage as hydrogen.* Energy Conversion, IEEE Transactions on, 2004. **19**(3): p. 633-640.
26. Loyd R. J, S.S.M., Nakamura T, Lieurance D. W, Hilal M. A, Rogers J. D, Purcell J. R, Hassenzahl W. V, *A feasible utility scale superconducting magnetic energy storage plant.* IEEE Trans. on Energy Conversion 1986: p. 63-68.
27. Aryan Nezhad, M., *Economic Impacts of Long-Term Wind Speed Changes on Optimal Planning of a Hybrid Renewable Energy System (HRES).* Journal of Solar Energy Research, 2021. **6**(1): p. 656-663.